6-1-2023

A pentasaccharide for monitoring pharmacodynamic response to gene therapy in GM1 gangliosidosis

Pamela Kell

Rohini Sidhu

Mingxing Qian

Sonali Mishra

Dennis J Dietzen

See next page for additional authors

Authors

Pamela Kell, Rohini Sidhu, Mingxing Qian, Sonali Mishra, Dennis J Dietzen, Jingqin Luo, Jean E Schaffer, Daniel S Ory, Xuntian Jiang, and et al.

A pentasaccharide for monitoring pharmacodynamic response to gene therapy in GM1 gangliosidosis

Pamela Kell,[a] Rohini Sidhu,[a,j] Mingxing Qian,[b] Sonali Mishra,[a] Elena-Raluca Nicoli,[c] Precilla D'Souza,[c,d] Cynthia J. Tifft,[c,d] Amanda L. Gross,[e] Heather L. Gray-Edwards,[e,k] Douglas R. Martin,[e] Miguel Sena- Esteves,[f] Dennis J. Dietzen,[g] Manmilan Singh,[h] Jingqin Luo,[i] Jean E. Schaffer,[a,l] Daniel S. Ory,[a,j] and Xuntian Jiang[a,*]

[a]Department of Medicine, Washington University School of Medicine, St. Louis, MO, 63110, USA
[b]Department of Developmental Biology, Washington University School of Medicine, St. Louis, MO, 63110, USA
[c]Medical Genetics Branch and Office of the Clinical Director, NHGRI, NIH, Bethesda, MD 20892, USA
[d]Office of the Clinical Director, NHGRI, NIH, Bethesda, MD, 20892, USA
[e]Scott-Ritchey Research Center, Auburn University College of Veterinary Medicine, Auburn, AL, 36849, USA
[f]Department of Neurology, Horae Gene Therapy Center, University of Massachusetts Medical School, Worcester, MA, 01605, USA
[g]Department of Pathology & Immunology, Washington University School of Medicine, St. Louis, MO, 63110, USA
[h]Department of Chemistry, Washington University, St. Louis, MO, 63130, USA
[i]Department of Surgery, Washington University School of Medicine, St. Louis, MO, 63110, USA

eBioMedicine
2023;92: 104627
Published Online 31 May 2023
https://doi.org/10.1016/j.ebiom.2023.104627

Summary

Background GM1 gangliosidosis is a rare, fatal, neurodegenerative disease caused by mutations in the GLB1 gene and deficiency in β-galactosidase. Delay of symptom onset and increase in lifespan in a GM1 gangliosidosis cat model after adeno-associated viral (AAV) gene therapy treatment provide the basis for AAV gene therapy trials. The availability of validated biomarkers would greatly improve assessment of therapeutic efficacy.

Methods The liquid chromatography-tandem mass spectrometry (LC-MS/MS) was used to screen oligosaccharides as potential biomarkers for GM1 gangliosidosis. The structures of pentasaccharide biomarkers were determined with mass spectrometry, as well as chemical and enzymatic degradations. Comparison of LC-MS/MS data of endogenous and synthetic compounds confirmed the identification. The study samples were analyzed with fully validated LC-MS/MS methods.

Findings We identified two pentasaccharide biomarkers, H3N2a and H3N2b, that were elevated more than 18-fold in patient plasma, cerebrospinal fluid (CSF), and urine. Only H3N2b was detectable in the cat model, and it was negatively correlated with β-galactosidase activity. Following intravenous (IV) AAV9 gene therapy treatment, reduction of H3N2b was observed in central nervous system, urine, plasma, and CSF samples from the cat model and in urine, plasma, and CSF samples from a patient. Reduction of H3N2b accurately reflected normalization of neuropathology in the cat model and improvement of clinical outcomes in the patient.

Interpretations These results demonstrate that H3N2b is a useful pharmacodynamic biomarker to evaluate the efficacy of gene therapy for GM1 gangliosidosis. H3N2b will facilitate the translation of gene therapy from animal models to patients.

Funding This work was supported by grants U01NS114156, R01HD060576, ZIAHG200409, and P30 DK020579 from the National Institutes of Health (NIH) and a grant from National Tay-Sachs and Allied Diseases Association Inc.

Keywords: Gene therapy; GM1 gangliosidosis; Pentasaccharide; Pharmacodynamic biomarker

Introduction

GM1 gangliosidosis is a rare, fatal, neurodegenerative genetic disease caused by mutations in the *GLB1* gene, resulting in deficiency of β-galactosidase enzyme activity and accumulation of glycoconjugates with a terminal β-galactose, including gangliosides GM1 and GA1, oligosaccharides, glycopeptides, and keratan sulfate.[1–3] GM1 gangliosidosis is estimated to affect 1 in

*Corresponding author.
E-mail address: jiangxuntian@wustl.edu (X. Jiang).
[j]Current address: Casma Therapeutics, Cambridge, MA 02139.
[k]Current address: Department of Radiology, Horae Gene Therapy Center, University of Massachusetts Medical School, Worcester, MA 01605.
[l]Current address: Joslin Diabetes Center, Harvard Medical School, Boston, MA 02215.

Research in context

Evidence before this study

GM1 gangliosidosis is a rare, fatal, neurodegenerative disease caused by mutations in the GLB1 gene, in which β-galactosidase enzyme activity is deficient, and glycoconjugates with a terminal β-galactose are accumulated. The successful delay of symptom onset, reduction of storage in the brain and peripheral tissues, and increase of lifespan in cat model by adeno-associated viral (AAV) gene therapy led to initiation of AAV gene therapy trials. Evaluation of treatment efficacy with clinical outcomes is difficult due to the small and heterogenous patient population as well as slower disease progression in the late-infantile and juvenile forms compared to the most severe, infantile form. Application of validated biomarkers would greatly improve assessment of therapeutic efficacy of the AAV gene therapy. Currently available biomarkers such as ganglioside GM1 in biofluids do not provide sufficient dynamic range to differentiate patients and control subjects, and thus their clinical applications are limited.

Added value of this study

In this study, we identified a pentasaccharide biomarker H3N2b that was markedly elevated in GM1 gangliosidosis patients and cats. After the standard compound of H3N2b was synthesized, the fully validated assays were developed to accurately determine this biomarker in biospecimens. Negative correlation between H3N2b levels and β-galactosidase enzyme activities was demonstrated. Consistent with improvement in neurological symptoms and lifespan, reduction of H3N2b in central nervous system, urine, plasma, and cerebrospinal fluid (CSF) samples from cats treated with IV AAV9 gene therapy was observed. The H3N2b levels in urine, plasma, and CSF samples from a patient receiving IV AAV9 gene therapy were also significantly reduced, in line with small and measurable improvements in clinical outcomes. The H3N2b pentasaccharide is a useful pharmacodynamic biomarker to translate gene therapy developed in cat model to patients and to monitor therapeutic response.

Implications of all the available evidence

H3N2b is a natural substrate of β-galactosidase and readily quantified in biofluids such as urine, plasma, and CSF, making it an ideal non-invasive pharmacodynamic biomarker for serially monitoring response to treatments that aim at restoration of β-galactosidase activity, such as gene therapy, marrow transplantation, pharmacological chaperones, and enzyme replacement therapy. The accurate measurement of H3N2b by the validated assays developed in this study allows us to implement this biomarker in expanded access study of gene therapy and the following Phase 1/2 trial and has implications for accelerating drug development in this rare genetic disease.

100,000–200,0000 live births.[2–4] The major clinical signs are progressive motor and cognitive decline, visual defects, and premature death. In addition to neurological manifestations, the disease also affects systemic organs, such as the liver, spleen, and skeletal structure. The clinical manifestations of GM1 gangliosidosis are heterogeneous, and the disease is divided into three categories based on the age of disease onset: type I (infantile form), type II (late-infantile and juvenile forms), type III (chronic or adult form), in which disease progression and severity of symptoms are in the order of type I > type II > type III. Over 200 mutations have been reported in *GLB1* and there is no clear correlation between genotype and phenotype.[2–4]

There are currently no effective therapies for GM1 gangliosidosis and only symptomatic treatments are available. In the GM1 gangliosidosis cat model, which faithfully recapitulates late-infantile or juvenile GM1 gangliosidosis, adeno-associated viral (AAV) gene therapy that restores β-galactosidase activity is the most promising treatment in delaying symptom onset, reducing lysosomal storage in the brain and peripheral tissues, and increasing lifespan.[5–7] These striking findings provided the foundation for initiation of two AAV gene therapy clinical trials (NCT03952637, NCT04273269), and a third AAV-based clinical trial also is underway (NCT04713475).[2] Evaluation of treatment efficacy with clinical endpoints is challenging due to the small and heterogeneous patient population, as well as slower progression in the non-infantile patients. Therefore, the use of validated biomarkers to predict clinical benefits is critical to accelerate drug development. The BEST-defined biomarker categories comprise susceptibility/risk biomarker, diagnostic biomarker, monitoring biomarker, prognostic biomarker, predictive biomarker, pharmacodynamic biomarker, safety biomarker, and surrogate endpoints.[8] Biomarkers are used in variety stages of drug development and serve multiple purposes, including 1) to monitor the safety of a therapy by safety biomarker; 2) to determine whether treatments provide desired effects by pharmacodynamic biomarker; 3) to predict patients who may respond better to intervention by predictive biomarker; 4) to predict clinical benefits more quickly than conventional clinical endpoints by surrogate endpoints. While monitoring biomarker overlaps with these 4 biomarkers, pharmacodynamic biomarkers that are proven to correlate with more clinically meaningful endpoints could theoretically be developed as the surrogate endpoints. Our goal is to identify pharmacodynamic biomarkers in readily accessible human biofluids such as urine, plasma, and cerebrospinal fluid (CSF) to facilitate monitoring of

treatment efficacy of gene therapy. Ideally, such biomarkers should show large dynamic range to differentiate the GM1 gangliosidosis and control subjects and be changed towards normal by effective treatment.

In this study, we evaluated the potential of ganglioside GM1 and oligosaccharides as pharmacodynamic biomarkers for gene therapy. Whereas ganglioside GM1 was moderately elevated in patient CSF and plasma, a pentasaccharide - referred as to H3N2b–was elevated more than 18-fold in patient CSF, plasma, and urine, and in the central nervous system (CNS) of the GM1 gangliosidosis cats. We identified its structure with mass spectrometry, chemical and enzymatic degradations; synthesized standard compound; developed fully validated assays; and confirmed its reduction in the CNS, urine, plasma, and CSF of GM1 gangliosidosis cats and in patient urine, plasma, and CSF in response to AAV gene therapy treatment, in agreement with improvement of lifespan and life quality in cats and clinical outcomes in a patient. These results suggest that H3N2b will be useful as an outcome measure for monitoring efficacy of gene therapy for GM1 gangliosidosis.

Methods

Study design

The goal of the study was to identify biomarkers for monitoring pharmacodynamic response to gene therapy in GM1 gangliosidosis. Samples from both patients and animal models were used in biomarker discovery as they offered complementary information and helped to validate potential biomarkers. The gene therapy was originally developed in a cat model, and the biomarkers validated in both patients and GM1 gangliosidosis cats are useful for translating the gene therapy from cats to patients. The plasma, CSF, and urine samples from GM1 gangliosidosis patients in a natural history study (NCT00029965) and a patient in the expanded access program of intravenous (IV) gene transfer vector AAV9/*GLB1* for GM1 gangliosidosis (19-HG-9958; NCT03952637), and age and gender-matched control subjects were obtained. The CNS, CSF, plasma, and urine samples were collected from normal, GM1 gangliosidosis, and AAV9 gene therapy treated GM1 gangliosidosis cats. Ganglioside GM1 and oligosaccharides were profiled in human biofluid samples from the natural history study, and two pentasaccharides H3N2a and H3N2b were selected as candidate biomarkers. Their structures were elucidated by tandem mass spectrometric assays and degradation studies. Only H3N2b was detectable in GM1 gangliosidosis cat model, which was chosen for further development. The response of H3N2b to AAV gene therapy in cat model and patient was confirmed after its standard compound and internal standard were synthesized, and fully validated assays were developed.

Chemicals and reagents

The formic acid (catalog number: 27001-1L-R), methanol (catalog number: 1060354000), acetonitrile (catalog number: AX0156-1), diethylamine (catalog number: 31730-250ML), 2-AA (catalog number: 10680-100G), $NaBH_3CN$ (catalog number: 918830-100G), methyl tert-butyl ether (MTBE) (catalog number: 650560-4L), $NaIO_4$ (catalog number: 311448-5G), sodium borohydride ($NaBH_4$) (catalog number: 213462-25G), ammonium acetate (catalog number: 73594-25G-F), ammonium hydroxide solution (catalog number: 338818-100ML), ethylene glycol (catalog number: 324558-100ML), acetic acid (catalog number: 695092-100ML), silver triflate (catalog number: 483346-5G), sodium methoxide (catalog number: 164992-100G), ethylenediamine (catalog number: 03550-250ML), acetic anhydride (catalog number: 320102-100ML), d6-acetic anhydride (catalog number: 175641-5G), pyridine (catalog number: 270970-100ML), ammonia (catalog number: 294993-170G), sodium (catalog number: 483745- 100G), and zinc chloride (catalog number: Z0152-50G) were purchased from Sigma-Aldrich (St. Louis, MO). The β(1-4)-galactosidase (streptococcus pneumoniae) (catalog number: GKX-5014), β-N-acetylhexosaminidase (recombinant from streptococcus pneumoniae, expressed in *E. coli*) (catalog number: GK80050), α(1-2,3,6)- mannosidase (Jack Bean) (catalog number: GKX-5010), and β-mannosidase (*Helix pomatia*) (catalog number: GKX-5015) were purchased from ProZyme (Hayward, CA). The d_3-GM1 (18:0) (catalog number: 2050) was provided by Matreya (State College, PA). Milli-Q ultrapure water was prepared in-house with a Milli-Q Integral Water Purification System (Billerica, MA).

Human subjects

De-identified urine, plasma, and CSF samples were collected from GM1 gangliosidosis natural history study (NCT00029965) at NHGRI and from the expanded access of IV gene transfer vector AAV9/*GLB1* (19-HG-9958; NCT03952637) at NHGRI. Control urine, plasma, and CSF samples were obtained from anonymized residual samples at St. Louis Children's Hospital. The GM1 gangliosidosis patients were diagnosed with genetic testing and β-gatactosidase activity. The control subjects were confirmed based on the medical record. Each GM1gangliosidosis case was matched to controls by age varying within 3 years old and gender. The larger control group sizes were used in the evaluation of ganglioside GM1 in plasma and CSF, discovery of oligosaccharide biomarkers in CSF, establishment of H3N2b reference ranges of urine, plasma, and CSF, as more control samples were available, though not all the additional controls met age requirement. In all the cohorts, the patient age and gender distributions were not found to be significantly different from those of the control groups ($p > 0.05$). The demographic characteristics of human subjects are given in Table 1.

Cohort	Sample type	Patient type	GM1 gangliosidosis	Control	p value
Evaluation of ganglioside GM1	Plasma	Age (range, median; mean ± SD)	3–20, 11; 11 ± 6.2	1–18, 10; 9 ± 5.6	0.3130[a]
		Male/Female (n/n)	5/5	20/10	0.5716[b]
		Late infantile (n)	4		–
		Juvenile (n)	6		–
	CSF	Age (range, median)	3–20, 11; 11 ± 6.2	<1–20, 6; 8 ± 6.4	0.151[c]
		Male/Female (n/n)	5/5	9/11	1[b]
		Late infantile (n)	4		–
		Juvenile (n)	6		–
Discovery of oligosaccharide biomarkers	Urine	Age (range, median)	3–20, 11; 11 ± 6.2	1–17, 13; 12 ± 4.9	0.7178[c]
		Male/Female (n/n)	5/5	5/5	1[b]
		Late infantile (n)	4		–
		Juvenile (n)	6		–
	Plasma	Age (range, median)	3–20, 11; 11 ± 6.2	1–18, 11; 10 ± 6.3	0.7038[a]
		Male/Female (n/n)	5/5	5/5	1[b]
		Late infantile (n)	4		–
		Juvenile (n)	6		–
	CSF	Age (range, median)	3–20, 11; 11 ± 6.2	<1–20, 6; 8 ± 6.4	0.151[a]
		Male/Female (n/n)	5/5	9/11	1[b]
		Late infantile (n)	4		–
		Juvenile (n)	6		–
Establishment of H3N2b reference range	Urine	Age (range, median)	3–20, 11; 11 ± 6.2	<1–26, 10; 10 ± 7.0	0.4615[a]
		Male/Female (n/n)	5/5	19/44	0.3797[b]
		Late infantile (n)	4		–
		Juvenile (n)	6		–
Establishment of H3N2b reference range	Plasma	Age (range, median)	3–20, 11; 11 ± 6.2	<1–23, 9; 9 ± 5.9	0.3095[a]
		Male/Female (n/n)	5/5	21/29	0.9072[b]
		Late infantile (n)	4		–
		Juvenile (n)	6		–
Establishment of H3N2b reference range	CSF	Age (range, median)	3–20, 11; 11 ± 6.2	<1–19, 8; 9 ± 6.6	0.225[a]
		Male/Female (n/n)	5/5	18/14	1[b]
		Late infantile (n)	4		–
		Juvenile (n)	6		–
Single patient in expanded access	Urine, plasma, CSF	Age	10		–
		Gender	Female		–
		GM1 gangliosidosis type	Juvenile		–
		Dose	1.5×10^{13} vg/kg		–

[a]Mann–Whitney U-test. [b]Chi-square test. [c]Two sample t-test.

Table 1: **Demographic characteristics of human subjects.**

Experimental animals

GM1 gangliosidosis and normal Siamese cats were used in the study. The AAV9 backbone expressing feline β-galactosidase contained a hybrid chicken β-actin (CBA) promoter, including the CMV immediate-early enhancer fused to the CBA promoter.[5] Treatment of GM1 gangliosidosis cats with IV AAV9 gene therapy and collection of brain stem, cerebellum, spinal cord (cervical intumescence, lumbar intumescence), frontal cortex, occipital cortex, parietal cortex, temporal cortex, and thalamus, plasma, CSF, and urine were described previously.[7] GM1 gangliosidosis cats were treated with an AAV9 vector expressing feline β-galactosidase (1.5×10^{13} vector genomes/kg body weight) by injection of the cephalic vein at a presymptomatic time point of ~1 month of age. The treated animals were randomly selected from a group of pooled GM1 gangliosidosis cats. The humane endpoint was defined by an animal's inability to stand on 2 consecutive days. Untreated GM1 gangliosidosis cats survived to 8.0 ± 0.6 months old, while treated GM1 cats lived to ~3.5 years. Age-matched normal cats were used as control. Animals were euthanized by pentobarbital overdose according to guidelines of the American Veterinary Medical Association. CSF was collected from the cisterna magna. Blood was drawn from a

peripheral vein and aliquoted into tubes with EDTAK2 for separation of plasma. Urine was collected directly from the bladder during the necropsy procedure. Postmortem tissue samples were removed according to standard protocol. Body fluid and tissue samples for biomarker analysis were frozen immediately in liquid nitrogen and stored at –80 °C until use.

Our pilot study demonstrated a significant difference between GM1 gangliosidosis and control subjects, with a >18- fold change and a small coefficient of variation (CV) of <15%, indicating a large effect size. To determine the minimum detectable effect size (strictly standardized mean difference) required to achieve 80% power at an alpha of 5% using a two-sided two-sample t-test, we calculated a range of sample sizes per group. Our results showed that a sample size of 4 per group was needed to detect an effect size of 2.38 with 80% power. For the discovery of oligosaccharide biomarkers, CNS samples were collected from 4 normal (2 males and 2 females) and 4 untreated GM1 gangliosidosis cats (2 males and 2 females). To evaluate the response of H3N2b to IV gene therapy treatment, CNS samples were collected from 4 normal (2 males and 2 females), 5 treated GM1 gangliosidosis (3 males and 2 females), and 4 untreated GM1 gangliosidosis cats (2 males and 2 females); CSF samples were collected from 12 normal (6 males and 6 females), 6 treated GM1 gangliosidosis (3 males and 3 females), and 7 untreated GM1 gangliosidosis cats (4 males and 3 females); plasma samples were collected from 12 normal (6 males and 6 females), 6 treated GM1 gangliosidosis (3 males and 3 females), and 8 untreated GM1 gangliosidosis cats (4 males and 4 females). However, we were able to collect urine samples from only 2 treated cats, and this sample size was not sufficient to assess the change of urine H3N2b in treated cats. No animals and samples were excluded. The investigators were not blind to the normal, untreated GM1 gangliosidosis, and treated GM1 gangliosidosis due to overt behavioral differences observed across 3 animal groups.

Ethics

Human studies adhered to the principles of the Declaration of Helsinki, as well as to Title 45, US Code of Federal Regulations, Part 46, Protection of Human subjects. Collection and analysis of de-identified human samples were approved by the institutional review boards at Washington University (202007152) and NHGRI (02-HG-0107 and 19-HG-9958), and consent forms were signed by all participants or their guardians. GM1 gangliosidosis and normal cats were raised at Auburn University College of Veterinary Medicine. All animal procedures were approved by the Institutional Animal Care and Use Committee at Auburn University and performed in accordance with the protocols of the National Research Council committee regarding the international guidelines for care and use of laboratory animals in research and ARRIVE guidelines for reporting animal experiments.

Analysis of H3N2b in urine, plasma, and CSF samples from patient in expanded access study and cat model

Validated methods (Supplementary Materials) were used to analyze patient samples. Samples consisting of calibration standards in duplicate, a blank, a blank with internal standard, quality control (QC) samples at the levels of low (LQC), middle (MQC), and high (HQC), and unknown clinical samples were analyzed. The total number of QC samples was at least 5% of that of unknown clinical samples. The study samples were randomized by assignment of temporary random numbers for LC-MS/MS run, and QC samples were randomly inserted into the study sample sequence. The standard curve covered the expected unknown sample concentration range, and samples that exceeded the highest standard could be diluted and re-assayed. In the dilution sample re-assay, a dilution QC (DQC) in triplicate was also included in the analytical run. The analysts were blind to the study sample identifications. The LC-MS/MS run acceptance criteria of FDA guidance[9] were met. The urine H3N2b was normalized to creatinine that was measured with procedure reported previously.[10] The same methods were used to analyze cat samples except that no QC samples were included in the LC-MS/MS runs. The H3N2b in cat tissues were normalized to tissue weights. The data were analyzed by the investigators who did not involve in the sample analysis.

Assays of β-galactosidase activity

The frozen sections (50 μm) were cut from cervical intumescence, frontal cortex, lumbar intumescence, and occipital cortex issue and homogenized manually in 50 mM citrate phosphate buffer, pH 4.4 (50 mM citric acid, 50 mM disodium hydrogen phosphate, 10 mM sodium chloride) containing 0.1% TritonX and 0.05% bovine serum albumin, followed by 2 freeze-thaw cycles and centrifugation at 15,700 g for 5 min at 4 °C. The activity of β-galactosidase in tissue homogenate or human CSF was measured using 4MU-β-D-galactoside incubated in citrate-phosphate buffer, pH 3.8, for 1 h, and fluorescence of cleaved 4MU was read on a Perkin-Elmer LS-5B luminescence spectrometer with excitation at 360 nm and emission at 450 nm. Protein concentrations in tissue homogenates were determined by a modification of the method of Lowry. The enzymatic activities in tissues and CSF were expressed as nmol 4MU/hr/mg protein and nmol 4MU/hr/mL, respectively.

Statistics

Statistical analyses of data were performed using GraphPad Prism software (version 9.0.0, GraphPad

Software Inc., San Diego, CA) and SAS (version 9.4, SAS Institute, Cary, NC). The data normality was assessed with Shapiro–Wilk test. Two sample t-test was employed to compare 2 groups with normal distribution. The nonparametric tests were used to analyze the data when not all the groups in the comparison were normally distributed. Mann–Whitney U-test was used to compare 2 groups. Kruskal–Wallis test, Dunn's multiple comparisons test as post hoc test, and Benjamini-Hochberg stepwise adjustment were used to compare more than 2 groups. Chi-square test was used to assess statistical significance of distributional differences between patient and control sex distributions. The inverse relationship between cat CNS H3N2b and β-galactosidase activity was fit by nonlinear regression using one phase decay least squares fit in GraphPad Prism and Spearman correlation coefficient was calculated to gauge the association. A p value of less than 0.05 was considered significant. The areas under receiver operating characteristic (ROC) curves (AUC) for human urine, plasma, and CSF were calculated and the optimal cutoffs with maximal Youden index were determine to discriminate GM1 gangliosidosis from control subjects.

Role of funders

The funders of this project played no role in the study design, execution of experiments, analysis and interpretation of data, preparation of the manuscript, and decision to submit manuscript.

Results

Ganglioside GM1 in human biofluids

A wide range of potential biomarkers have been explored in the GM1 gangliosidosis cat model to assess clinical efficacy of AAV gene therapy.[5,6,11,12] CSF ganglioside GM1 appeared the most promising exhibiting >30-fold elevation in untreated GM1 gangliosidosis cats, and reduction in response to AAV gene therapy treatment.[11] We compared ganglioside GM1 in plasma and CSF from type II GM1 gangliosidosis and control human subjects (Supplemental Materials: Biomarker discovery). The elevation in plasma ganglioside GM1 was less than 2-fold, with only the most abundant ganglioside GM1 species in the plasma, GM1 (16:0) (p = 0.012) and GM1 (18:0) (p = 0.022), showing significant elevation in GM1 gangliosidosis patients (Fig. 1a). These results were in agreement with only moderate elevation of ganglioside GM1 in dried blood spots from GM1

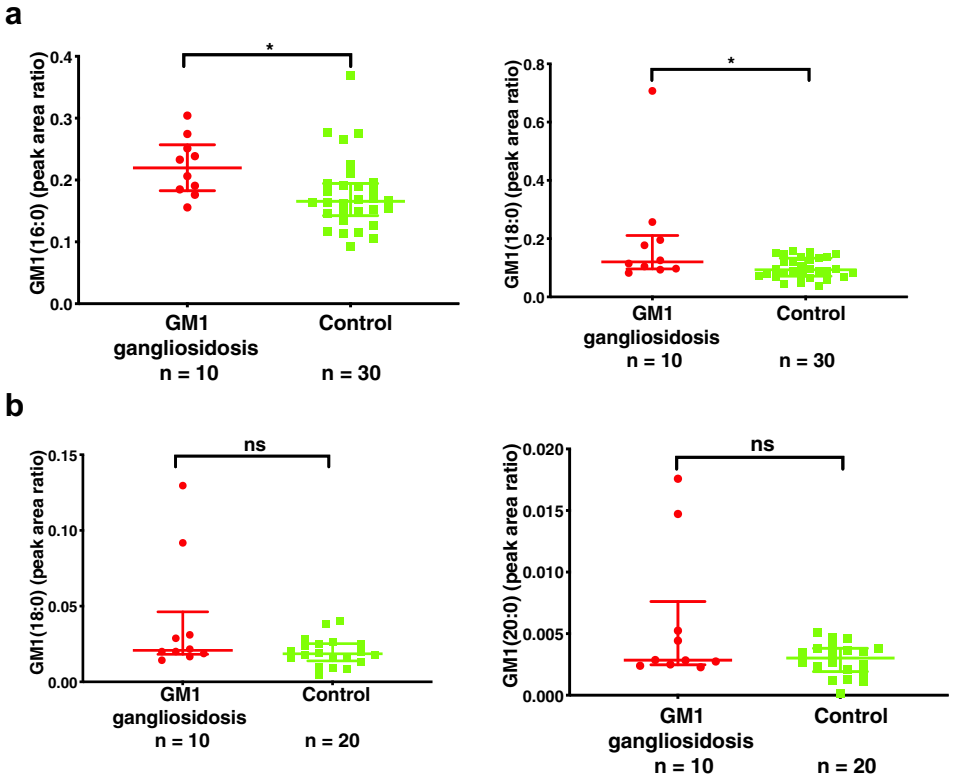

Fig. 1: **Ganglioside GM1 in human plasma and CSF.** (a) Ganglioside GM1 in human plasma samples. (b) Ganglioside GM1 in human CSF samples. Data are presented as median ± interquartile peak area ratio of analyte to internal standard. GM1 (16:0), C16:0 ganglioside GM1; GM1 (18:0), C18:0 ganglioside GM1; GM1 (20:0), C20:0 ganglioside GM1. The internal standard is d_3-GM1 (18:0). Mann–Whitney U-test was used to compare GM1 gangliosidosis and controls. ns: not significant; *: $p < 0.05$.

gangliosidosis patients.[13] By contrast, there were no significant differences in any of the ganglioside GM1 species in CSF between GM1 gangliosidosis patients and controls (Fig. 1b).

Discovery of oligosaccharides as GM1 gangliosidosis biomarkers

Several oligosaccharides have been found to be significantly elevated in urine from GM1 gangliosidosis patients and used for diagnosis of this disorder.[14–18] We profiled the oligosaccharides in urine, plasma and CSF samples (Supplemental Materials: Biomarker discovery). We developed a simple and sensitive liquid chromatography-tandem mass spectrometry (LC-MS/MS) method for profiling oligosaccharides, in which reductive amination of oligosaccharides with 2-aminobenzoic acid (2-AA) and sodium cyanoborohydride (NaBH3CN) was used to increase its retention on reversed-phase high performance liquid chromatography (HPLC) column and mass spectrometric sensitivity.[19]

We identified a pair of pentasaccharides (H3N2a and H3N2b) that were significantly elevated in GM1 gangliosidosis urine samples, where H is hexose, and N is N-acetylhexosamine. The pentasaccharides H3N2a and H3N2b were detectable in patient plasma and CSF (Fig. 2a). There are unknown interfering isomers (peak 1 and 3 in Fig. 2b) of H3N2a and H3N2b in human samples, which have not been reported previously. H3N2a and H3N2b were elevated >18-fold in urine ($p < 0.0001$ for H3N2a and H3N2b), plasma ($p < 0.0001$ for H3N2a and H3N2b), and CSF ($p < 0.0001$ for H3N2a and H3N2b) samples from type II (late infantile and juvenile) GM1 gangliosidosis patients (Fig. 3a and b). We further found that the H3N2b but not H3N2a was detectable and elevated in the CNS of the GM1 gangliosidosis cat model, and brain stem as an example shown in Fig. 2a). H3N2b was barely detectable in CNS of normal cat and accumulated in all of these regions of the GM1 gangliosidosis cat CNS, including brain stem ($p = 0.0217$), cerebellum ($p = 0.0217$), spinal cord (cervical intumescence ($p = 0.0217$), lumbar intumescence ($p = 0.0217$)), frontal cortex ($p = 0.0217$), occipital cortex ($p = 0.0217$), parietal cortex ($p = 0.0217$), temporal cortex ($p = 0.0217$), and thalamus regions ($p = 0.0217$) (Fig. 3c). The finding that H3N2b is a common biomarker for the cat model and for GM1 gangliosidosis patients suggests that this pentasaccharide may be able to assist in the translation of new treatments from the cat model into patients.

Structural identification of H3N2a and H3N2b

The H3N2a and H3N2b oligosaccharides were detected previously in urine from patients with GM1 gangliosidosis disease and Morquio B syndrome and characterized as underivatized-[20,21] and permethylated-oligosaccharides[22] on different MS platforms. Only the structure of H3N2a isolated from the urine of a Morquio B patient had been confirmed with proton nuclear magnetic resonance spectroscopy (^{1}HNMR).[23] To obtain structural information for the biomarkers, 2-AA-H3N2a and 2-AA-H3N2b were isolated from HPLC fractions. We found that structural information obtained from underivatized-[20,21] and permethylated-forms[22] was different from 2-AA derivatives. We performed rigorous structure characterization to identify the structures of H3N2a and H3N2b, including tandem mass spectrometry, chemical and enzymatic degradations (Supplemental Materials: Structure identification of pentasaccharides). The product ion spectra (Fig. 2b, Figs. S1a and S2) of $[M+H]^+$, $[M-H]^-$, and $[M+Na]^+$ ions of 2-AA derivatives indicate that the sequences of both oligosaccharides are ^{5}Hexose-^{4}N-acetylhexosamine-^{3}Hexose-^{2}Hexose-^{1}N-acetylhexosamine. Sodium periodate ($NaIO_4$) oxidation products of 2-AA-H3N2a and 2-AA-H3N2b suggested that the linkages of H3N2a and H3N2b were ^{5}Hexose-(1 → 4)-^{4}N-acetylhexosamine-(1 → 2)-^{3}Hexose-(1 → 6)-^{2}Hexose-(1 → 4)-^{1}N-acetylhexosamine and ^{5}Hexose-(1 → 4)-^{4}N-acetylhexosamine-(1 → 2)-^{3}Hexose-(1 → 3)-^{2}Hexose-(1 → 4)-^{1}N-acetylhexosamine, respectively (Figs. S1b, 1c and S3). The stepwise digestion of 2-AA-H3N2a and 2-AA-H3N2b with β1,4-galactosidase, β-N-acetylglucosaminidase, α-1-2,3,6-mannosidase, and β-mannosidase confirmed the H3N2a and H3N2b were ^{5}galactose-(β1 → 4)-^{4}N-acetylglucosamine-(β1 → 2)-^{3}mannose-(α1 → 6)-^{2}mannose-(β1 → 4)-^{1}N-acetylhexosamine and ^{5}galactose-(β1 → 4)-^{4}N-acetylglucosamine-(β1 → 2)-^{3}mannose-(α1 → 3)-^{2}mannose-(β1 → 4)-^{1}N-acetylhexosamine, respectively (Figs. S1d and S4). The reducing terminus of both 2-AA-H3N2a and 2-AA-H3N2b was identified as 2-AA-N-acetylglucosamine that was confirmed with a standard compound. The H3N2a and H3N2b were identified as O-β-D-galactopyranosyl-(1 → 4)-O-(2-acetamido-2-deoxy-β-D-glucopyranosyl)-(1 → 2)-O-α-D-mannopyranosyl-(1 → 6)-O-β-D-mannopyranosyl-(1 → 4)-2- acetamido-2-deoxy-α,β-D-glucopyranose and O-β-D-galactopyranosyl-(1 → 4)-O-(2-acetamido-2-deoxy-β-D-glucopyranosyl)-(1 → 2)-O-α-D-mannopyranosyl-(1 → 3)-O-β-D-mannopyranosyl-(1 → 4)-2-acetamido-2-deoxy-α,β-D-glucopyranose, respectively. They are moieties of complex N-glycan.

Synthesis of H3N2b and d_6-H3N2b

We chose H3N2b for further biomarker development, which is the common biomarker observed in the GM1 cat model and patients. As no commercial reference standard of H3N2b and its stable isotope-labeled analog as internal standard were available, we synthesized H3N2b and d_6-H3N2b from acceptor **1**[24] and donor **3**[25] in 23% and 16.5% overall yields over 5 steps, respectively (Fig. 4a; Supplemental Materials: Synthesis of H3N2b). H3N2b and d_6- H3N2b with chromatographic

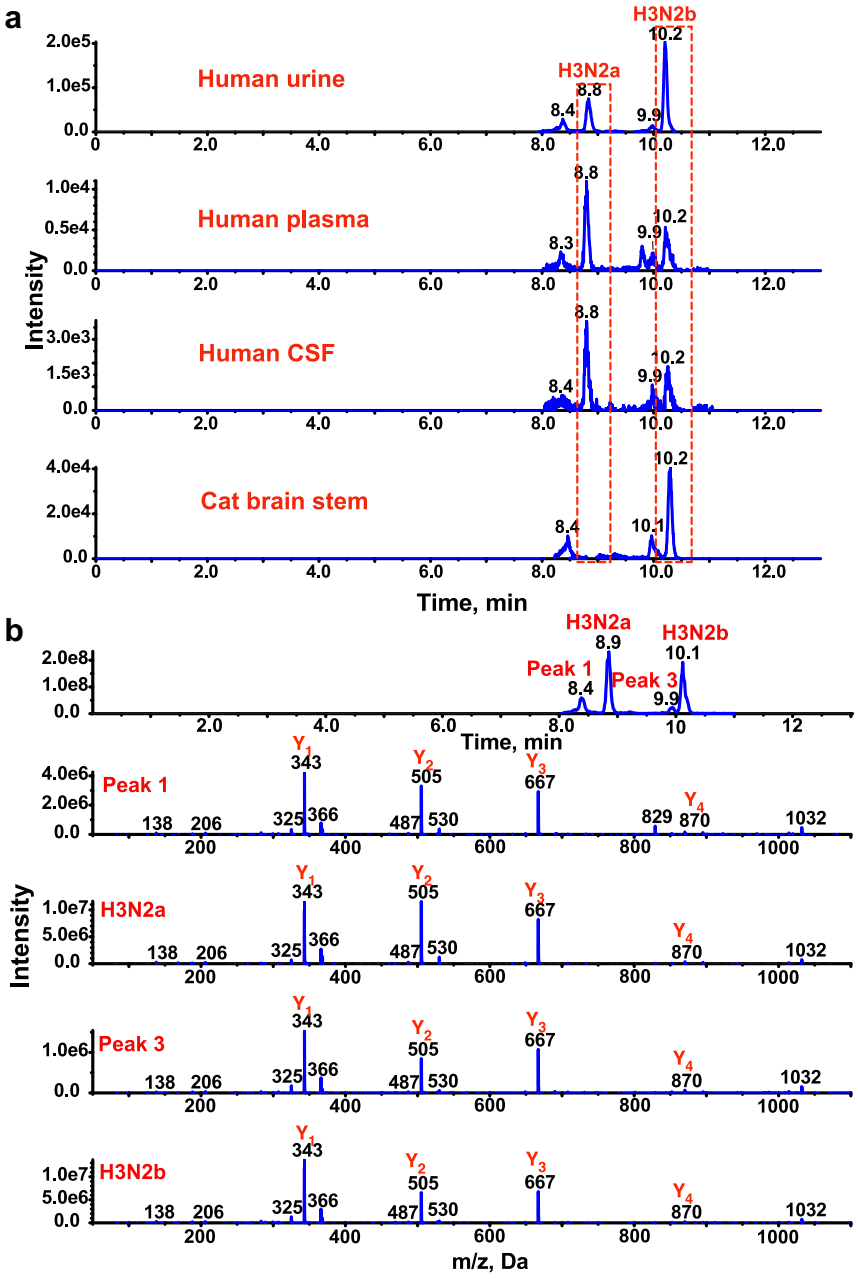

Fig. 2: **Separation of H3N2a and H3N2b.** (a) Chromatograms of 2-AA derivatized H3N2a and H3N2b in type II GM1 gangliosidosis human urine, plasma, CSF, and cat brain stem samples. H3N2a is not found in the cat with brain stem as an example. (b) Enhanced product ion spectra of $[M+H]^+$ ions of 2-AA derivatized H3N2a, H3N2b, and 2 interfering peaks (peaks 1 and 3) show that they are isomeric pentasaccharides.

purity >99% (H3N2b is shown in Fig. 4b) were obtained after purification with HPLC, which were determined after derivatization with 2-AA. The retention time and tandem mass spectrum of synthetic H3N2b were the same as endogenous H3N2b (Fig. 4c; Supplemental Materials: Confirmation of H3N2b structure) after derivatization with 2-AA, confirming the proposed structure of H3N2b.

Validation of LC-MS/MS assays for determination of H3N2b in human urine, plasma, and CSF

After synthesis of H3N2b and internal standard d_6-H3N2b, we further optimized the LC-MS/MS conditions and validated the methods for quantification of H3N2b in human urine, plasma, and CSF according to FDA Bioanalytical Method Validation Guidance.[9] As H3N2b is an endogenous analyte, we used water as a

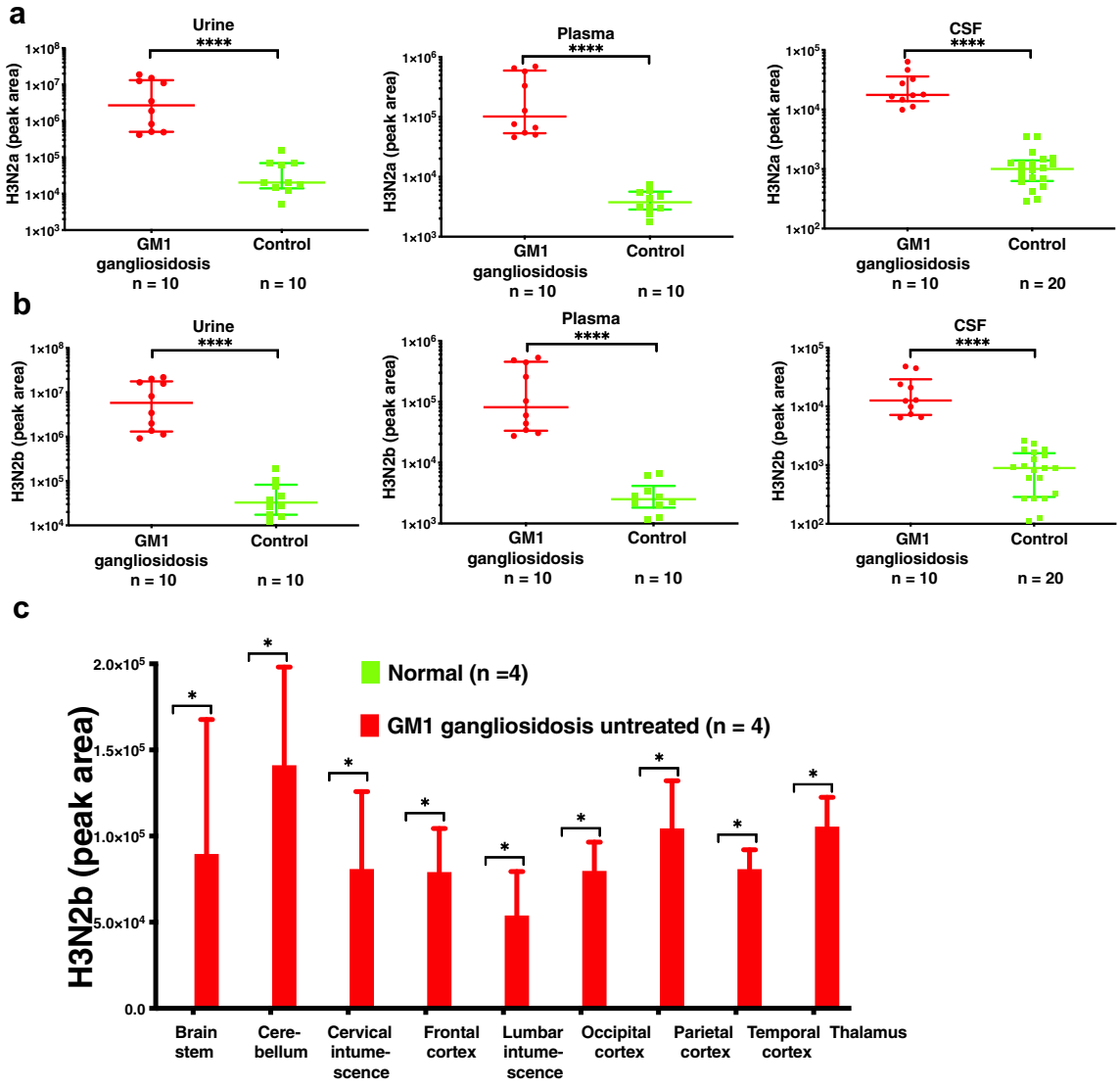

***Fig. 3:* Discovery of pentasaccharide biomarkers H3N2a and H3N2b.** (a) H3N2a in human urine, plasma, and CSF samples. Data are presented as median ± interquartile area on log scale. Mann–Whitney U-test was used to compare GM1 gangliosidosis and controls. (b) H3N2b in human urine, plasma, and CSF samples. Data are presented as median ± interquartile peak area on log scale. Mann–Whitney U-test was used to compare GM1 gangliosidosis and controls. (c) H3N2b in cat CNS samples. In normal cats, H3N2b was undetectable. Data are presented as mean ± standard deviation. Comparison of normal and untreated GM1 gangliosidosis was performed with Wilcoxon rank sum test. *: $p < 0.05$; **: $p < 0.01$; ***: $p < 0.001$; ****: $p < 0.0001$.

surrogate matrix for standard curves for urine, plasma, and CSF.[26] The methods showed good linearity and parallelism, selectivity and specificity, sensitivity, accuracy, precision, and reproducibility, stability, carryover, and dilution integrity (Supplemental Materials: Method Validation for H3N2b in human urine, plasma, and CSF). The validated methods allowed us to reliably quantify H3N2b in clinical biospecimens.

Establishment of normal cutoffs for human urine, plasma, and CSF H3N2b

We analyzed urine samples from 10 untreated GM1 gangliosidosis patients and 63 control subjects, plasma samples from 10 untreated GM1 gangliosidosis patients and 50 control subjects, and CSF samples from 10 untreated GM1 gangliosidosis patients and 32 control subjects. The reference ranges for GM1 gangliosidosis urine, control urine, GM1 gangliosidosis plasma,

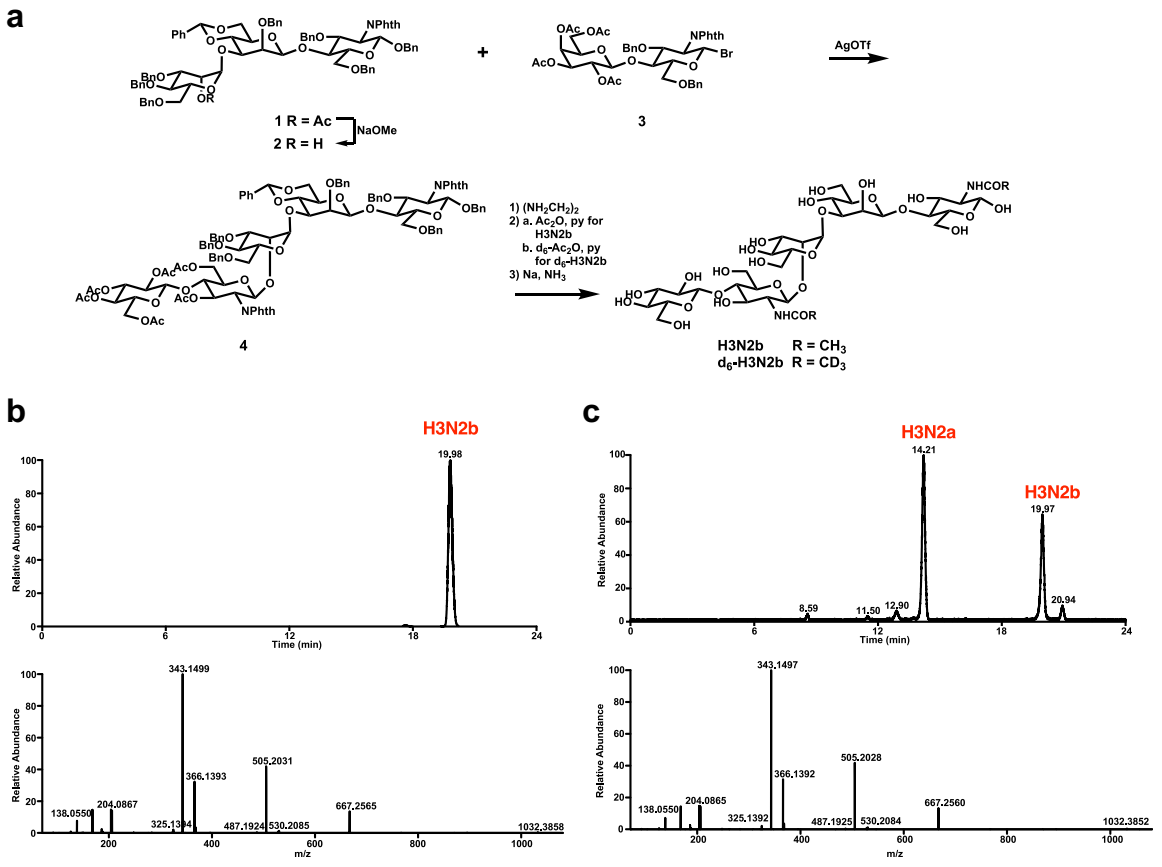

***Fig. 4:* Synthesis of H3N2b and its internal standard and confirmation of H3N2b structure.** (a) Synthesis of H3N2b and d6-H3N2b. (b) Chromatogram (detected by product ion scan) and product ion spectra of [M+H]+ ion of 2-AA derivatized synthetic H3N2b after purification with HPLC. (c) Chromatogram (detected by product ion scan) and product ion spectra of $[M+H]^+$ ion of 2-AA derivatized H3N2b in GM1 gangliosidosis urine.

control plasma, GM1 gangliosidosis CSF, and control CSF, were 1.54–60.8 ng/μg creatinine, 0.004–8.04 ng/μg creatinine, 11.1–134 ng/mL, <1–4.88 ng/mL, 4.4–59.3 ng/mL, and <1–8.84 ng/mL, respectively (Fig. 5a–c). The cut-offs of 0.98 ng/μg creatinine, 8.0 ng/mL, and 3.5 ng/mL for urine, plasma, and CSF were established from ROC curves. Sensitivities of 96.8%, 100%, and 96.9% were obtained to distinguish GM1 gangliosidosis from control based on urine, plasma, and CSF H3N2b, respectively. Specificities of 100% were observed using urine, plasma, and CSF H3N2b cutoffs (Fig. 5d–f). The excellent diagnostic accuracies and specificities of urine, plasma, and CSF assays were demonstrated by AUC that are close to 1. While there was no significant correlation between age and H3N2b levels within late infantile or juvenile group (Fig. 5g), late infantile patients showed higher H3N2b levels compared to juvenile patients ($p = 0.00095$ for urine; $p = 0.019$ for plasma; $p = 0.0039$ for CSF) (Fig. 5h). Lower residual β-galactosidase enzyme activity was reported in late infantile compared to juvenile patients,[27] suggesting that the H3N2b levels are negatively correlated with residual β-galactosidase enzyme activity. There was no significant difference in H3N2b levels between male and female patients (Fig. S5).

Pharmacodynamic response of H3N2b to AAV9 gene therapy in GM1 gangliosidosis cat model

IV administration of AAV9 vectors encoding feline β-galactosidase to GM1 gangliosidosis cat model led to profound increases in lifespan and quality of life.[7] Treated GM1 cats had clear preservation of brain architecture and metabolite levels as assessed by MRI and MRS, respectively. β-galactosidase activity reached carrier levels in the cerebrum and normal to above-normal levels in the cerebellum and spinal cord. Reduction of storage material to near-normal levels was shown throughout the central nervous system and liver. Reduced microgliosis and astrocytosis also were documented in treated GM1 animals. We used H3N2b to

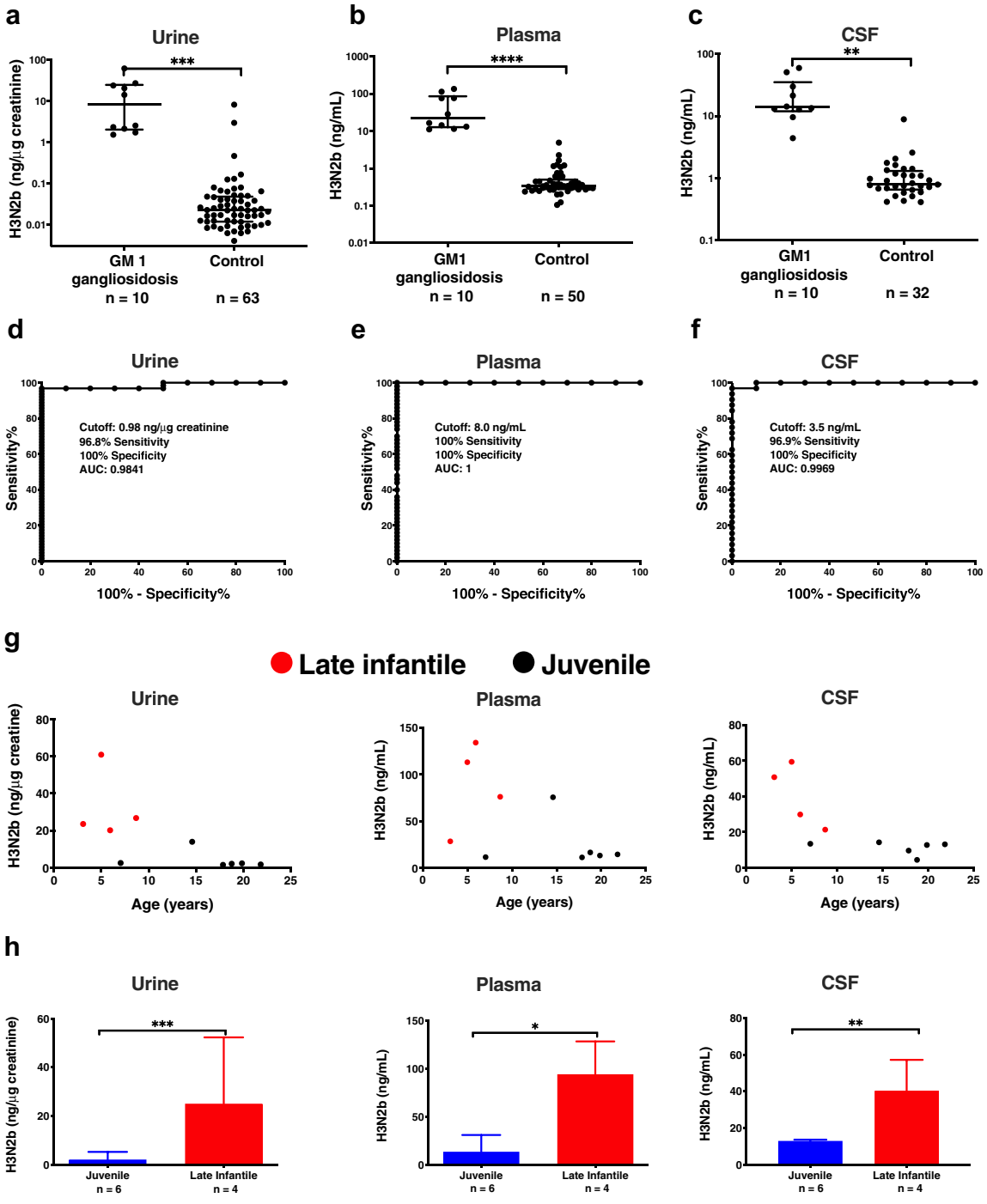

Fig. 5: **H3N2b in human urine, plasma, and CSF.** (a) H3N2b normalized to creatinine in human urine samples. H3N2b concentrations are presented as median ± interquartile on log scale. Mann–Whitney U-test was used to compare GM1 gangliosidosis and controls. (b) H3N2b concentrations in human plasma samples. The measured H3N2b concentrations that were below the lower limit of quantification (LLOQ, 1 ng/mL) were used for purpose of plotting, though the CV and relative error (RE) for these samples may not meet acceptance criteria for the validated assay. H3N2b concentrations are presented as median ± interquartile on log scale. Mann–Whitney U-test was used to compare GM1 gangliosidosis and controls. (c) H3N2b concentrations in human CSF samples. The measured H3N2b concentrations that were below the LLOQ (1 ng/mL) were used for purpose of plotting, though the CV and RE for these samples may not meet acceptance criteria for the validated assay. H3N2b concentrations are presented as median ± interquartile on log scale. Mann–Whitney U-test was used to compare GM1 gangliosidosis and

assess AAV9 gene therapy treatment efficacy in cat CNS. The H3N2b was significantly reduced after AAV9 gene therapy treatment in all regions: brain stem ($p = 0.0431$), cerebellum ($p = 0.0325$), cervical intumescence ($p = 0.0306$), lumbar intumescence) ($p = 0.0306$), frontal cortex ($p = 0.0469$), occipital cortex ($p = 0.0429$), parietal cortex ($p = 0.0431$), temporal cortex ($p = 0.0306$), and thalamus regions ($p = 0.0306$) (Fig. 6a). An inverse correlation between H3N2b levels and β-galactosidase enzyme activities was observed in cat cervical intumescence, lumbar intumescence, frontal cortex, and occipital cortex where the enzymatic activity data were available (Fig. 6b). Consistent with reduction of H3N2b in CNS, the CSF H3N2b was significantly reduced in treated GM1 gangliosidosis cats ($p = 0.0350$) (Fig. 6c). Reduction of plasma ($p = 0.0350$) (Fig. 6d) and urine (statistical analyses were not performed due to only 2 treated urine samples available) (Fig. 6e) H3N2b levels were also observed, in line with the restoration of β-galactosidase activity in peripheral organs.[7]

Pharmacodynamic response of H3N2b to AAV9 gene therapy in GM1 gangliosidosis patient

To evaluate the response of H3N2b to IV AAV9-mediated *GLB1* gene therapy in a GM1 gangliosidosis patient, we analyzed H3N2b levels in pre- and post-treatment urine, plasma, and CSF samples collected from a juvenile onset child who received the treatment under an expanded access protocol (19-HG-9958; NCT03952637). Significant decreases in urine, plasma, and CSF H3N2b were detectable by 0.5, 3, and 3 months after treatment, respectively (Fig. 7a–c). Urine, plasma, and CSF H3N2b levels were reduced 68%, 61%, and 59% at the last time point, respectively. The plasma H3N2b level was decreased to the normal range (derived in Fig. 5). In parallel with reduction of CSF H3N2b, the CSF β-galactosidase activity was increased (Fig. 7d). This patient showed small improvements on the Vineland Adaptive Behavior Scale Version V. 3, in total brain volume by magnetic resonance imaging (MRI), and on the Clinical Global Impressions Scale. She was stable on floor and upright mobility assessments. These data indicate that gene therapy to improve patient outcomes was accompanied by significant changes of the H3N2b biomarker in both the CNS and somatic tissues.

Discussion

Drug development in rare neurodegenerative diseases such as GM1 gangliosidosis is challenging due to the small and heterogeneous patient population as well as slow progression in the non-infantile patients. Use of non-invasive biomarkers is critical to accelerate treatment development. Numerous potential biomarkers for GM1 gangliosidosis have previously been reported[3,12,28–35] and several have been explored in the GM1 gangliosidosis cat model to assess response to therapy.[7,11,12] Of these, CSF ganglioside GM1 appeared the most promising, exhibiting more than 30-fold elevation in untreated GM1 gangliosidosis cats and reduction following AAV gene therapy treatment.[11] In the present study, however, we found that the application of ganglioside GM1 in clinical studies was limited by insufficient dynamic range between GM1 gangliosidosis and control, as there was less than 2-fold elevation in the CSF and plasma of GM1 gangliosidosis patients; there was overlap between GM1 gangliosidosis and controls, and GM1 in urine was undetectable. Given the advances in gene therapy for GM1 gangliosidosis, identification of additional clinically relevant biomarkers is urgently needed to assess treatment response.

Reports have shown that AAV gene therapy in the GM1 gangliosidosis cat model restored β-galactosidase activity, leading to extraordinary extension in lifespan and improvement of neurological symptoms.[5,7,12] Based on these preclinical results, the Phase 1/2 clinical trial of IV AAV9 gene therapy (NCT03952637) for type I and II GM1 gangliosidosis was initiated in May 2019, and intracisternal AAVrh10 (NCT04273269) and AAVHu68 (NCT04713475) gene therapies for type I and II GM1 gangliosidosis are underway. To facilitate the translation of AAV gene therapy developed in animal models to patients, we undertook biomarker discovery efforts in this disorder. Since oligosaccharides had been shown previously to be significantly elevated in urine from GM1 gangliosidosis patients,[14–18] we profiled oligosaccharides in biospecimens from a natural history study at NIH (NCT00029965) and the GM1 gangliosidosis cat model. We found two pentasaccharides, H3N2a and H3N2b, that were elevated >18-fold in human plasma, CSF, and urine. For reasons yet to be determined, however, only H3N2b was detectable in the CNS of the GM1 gangliosidosis cats. H3N2b is a potential translatable biomarker for assessing AAV treatment efficacy in the cat model and patients. These pentasaccharides had previously been proposed as diagnostic biomarkers.[14–18]

However, due to lack of authentic standards, ill-defined structures and detection of H3N2a and H3N2b as a mixture, the oligosaccharide assays were semi-quantitative and no reference ranges were established, which limited their utility as pharmacodynamic biomarkers. Here, preliminary assignments of

controls. (d) Determination of cutoff for urine using ROC curve. (e) Determination of cutoff for plasma using ROC curve. (f) Determination of cutoff for CSF using ROC curve. (g) Relations between urine, plasma, and CSF H3N2b and age/disease type. (h) Comparison of H3N2b in late infantile and juvenile GM1 gangliosidosis patients. Data are presented as mean ± standard deviation. Mann–Whitney U-test was used to compare late infantile and juvenile GM1 gangliosidosis patients. *: $p < 0.05$; **: $p < 0.01$; ***: $p < 0.001$; ****: $p < 0.0001$.

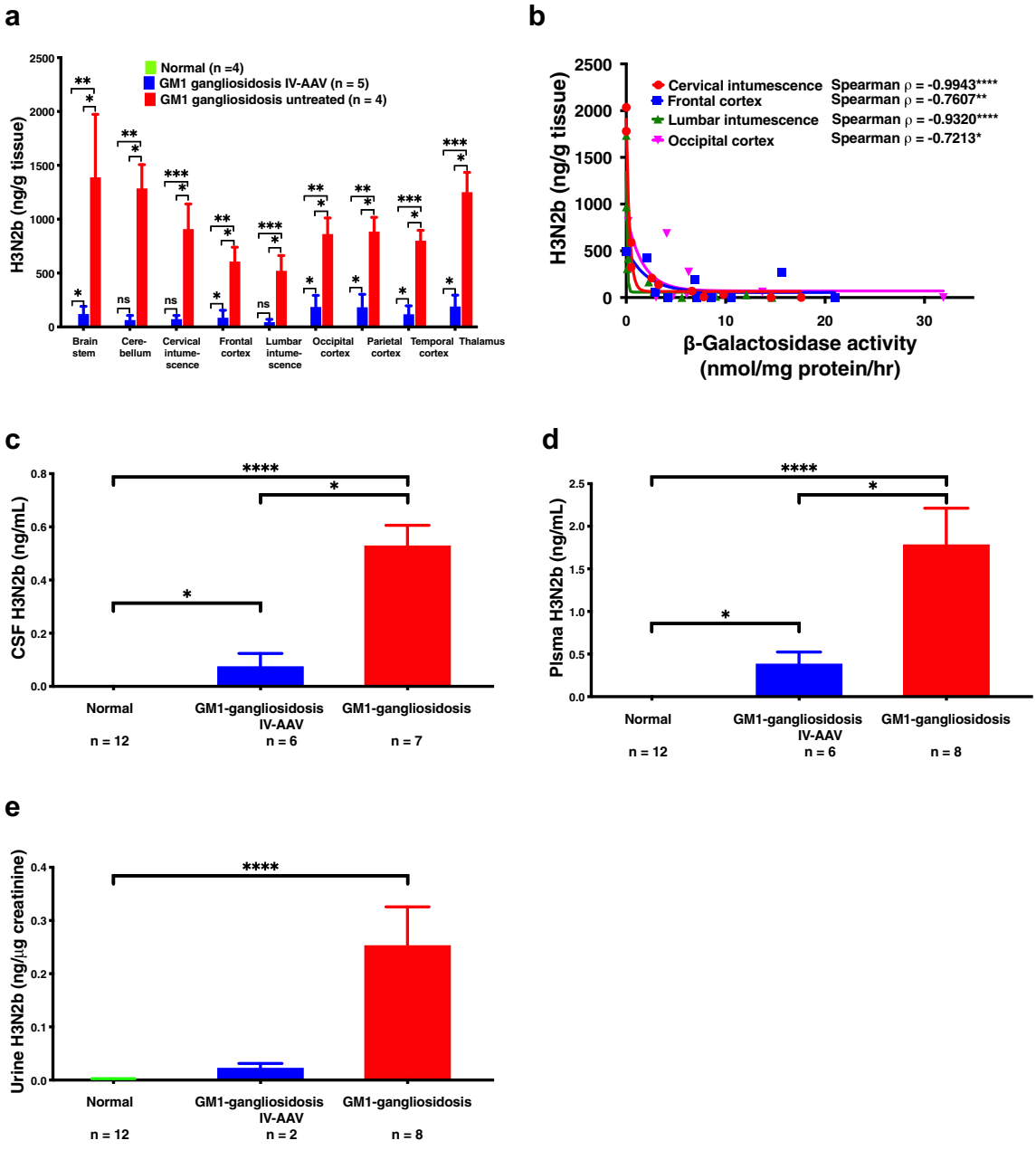

Fig. 6: **Response of H3N2b to IV AAV9 gene therapy in cat model.** (a) H3N2b in cat CNS samples. Data are presented as mean ± standard deviation. Comparison of normal, GM1 gangliosidosis treated with AAV gene therapy, and untreated GM1 gangliosidosis was performed with the Kruskal–Wallis test, Dunn's multiple comparisons test as post hoc test, and Benjamini-Hochberg stepwise adjustment. (b) Correlation of H3N2b in cat CNS with β-galactosidase activity. H3N2b level and β-galactosidase activity were fitted with nonlinear one phase decay least squares fit, and Spearman rank based correlation coefficients indicate that they are negatively correlated. (c) H3N2b in CSF from normal cats, GM1 gangliosidosis cats treated with IV AAV9 gene therapy, and untreated GM1 gangliosidosis cats. H3N2b in CSF of normal cats was undetectable. Data are presented as mean ± standard deviation. Comparison of normal, GM1 gangliosidosis treated with AAV gene therapy, and untreated GM1 gangliosidosis was performed with the Kruskal–Wallis test, Dunn's multiple comparisons test as post hoc test, and Benjamini-Hochberg stepwise adjustment. (d) H3N2b in plasma from normal cats, GM1 gangliosidosis cats treated with IV AAV9 gene therapy, and untreated GM1 gangliosidosis cats. H3N2b in plasma of normal cats was undetectable. Data are presented as mean ± standard deviation. Comparison of normal, GM1 gangliosidosis treated with AAV gene therapy, and untreated GM1 gangliosidosis was performed with the Kruskal–Wallis test, Dunn's multiple comparisons test as post hoc test, and Benjamini-Hochberg stepwise adjustment. (e) H3N2b in urine normalized to creatinine from normal cats, GM1 gangliosidosis cats treated with IV AAV9 gene therapy, and untreated GM1 gangliosidosis cats. Data are

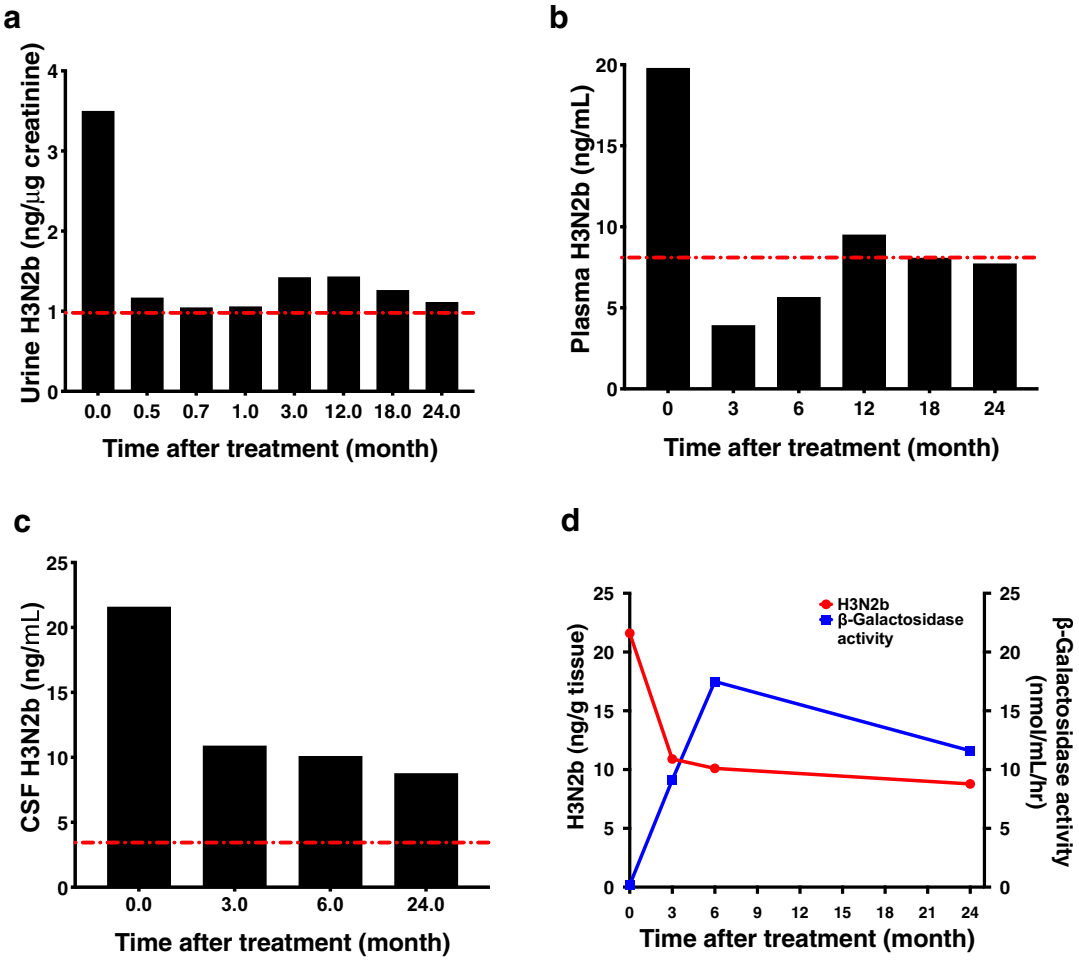

Fig. 7: **Response of H3N2b to IV AAV9 gene therapy in a GM1 gangliosidosis patient.** (a) H3N2b in urine. (b) H3N2b in plasma. (c) H3N2b in CSF. (d) Changes of CSF H3N2b and β-galactosidase activity. The red dash-dotted lines show the cutoffs for normal ranges as derived from ROC curve analysis.

the pentasaccharide structures were achieved through mass spectrometric analyses, chemical and enzymatic degradations, followed by synthesis of standard compound of H3N2b, and the proposed H3N2b structure was confirmed by comparison of endogenous and synthetic compounds using LC-MS/MS. Reliable H3N2b data can only be generated from bioanalytical methods after their selectivity, sensitivity, accuracy, precision, and stability are validated. The pure H3N2b as reference standard is a prerequisite to develop validated methods because it is used to prepare calibration standards and QC samples, which serve as reliable and consistent benchmarks for assessing the accuracy, precision, and sensitivity of the analytical methods. In addition, the use of H3N2b in bioanalytical methods allows for traceability and comparability of results across different laboratories and methods. This is particularly important in diagnosis and pharmacodynamic study in clinical trials. With synthetic H3N2b at hand, we developed fully validated assays to accurately quantify H3N2b in the samples collected from clinical studies and to establish the reference ranges for normal and GM1 gangliosidosis. This work paves the way for application of H3N2b as a pharmacodynamic biomarker for AAV gene therapy or any treatment that increases β-galactosidase activity.

The present study provides strong support for the H3N2b pentasaccharide as a pharmacodynamic biomarker for response to therapy in GM1 gangliosidosis

presented as mean ± standard deviation. Comparison of normal, GM1 gangliosidosis treated with AAV gene therapy, and untreated GM1 gangliosidosis was performed with the Kruskal–Wallis test, Dunn's multiple comparisons test as post hoc test, and Benjamini-Hochberg stepwise adjustment. Statistical analyses were not performed for the urine H3N2b in GM1 gangliosidosis cats treated with IV AAV9 gene therapy (n = 2). ns: not significant; *: $p < 0.05$; **: $p < 0.01$; ***: $p < 0.001$; ****: $p < 0.0001$.

patients. This natural substrate of β-galactosidase is elevated in GM1 gangliosidosis, and its level is inversely proportional to enzyme activity. We found that H3N2b levels were sharply reduced in the CNS of GM1ganglioidosis cats in response to IV AAV9 gene therapy, and this alternation was reflected in the CSF. The post-treatment reduction of H3N2b levels in cat plasma and urine most likely reflected the reduction of H3N2b in peripheral tissues. Furthermore, the application of biomarker can be translated to GM1 ganglisoidosis patients, as demonstrated by reduction of H3N2b in urine, plasma and CSF samples from the patient with improved clinical outcomes and increased CSF β-galactosidase activity after receiving IV AAV9-*GLB1* gene therapy. The reduction of CSF H3N2b is consistent with an ability of the AAV9 vector to cross blood brain barrier and transduce cells in the CNS following IV administration, strongly supporting that systemic AAV9 administration will be able to effectively restore functional β-galactosidase for the treatment of both the neurological and somatic disorders of GM1 gangliosidosis.[7] This contrasts with other GM1 gangliosidosis biomarkers that can only serve as either peripheral or CNS biomarkers.[3] Production of functional β-galactosidase by gene therapy is unable to reverse the damage that has already occurred in the nervous system, therefore we observed only small improvement of symptoms in the symptomatic patient receiving gene therapy. However, the treatment has the potential to slow down or halt the progression of the disease by preventing further damage as demonstrated in the study of cat model, and the quality of life of patient is improved.

This study has several limitations. First, consistent with the fact that gangliosidosis is an ultrarare disorder, it was challenging to collect sufficient samples to demonstrate the generalizability of study findings. In this study, we did not have access to samples from GM1 gangliosidosis type I (infantile) and III (adult) patients, who have lower and higher β-galactosidase activities than type II patients, respectively. In addition, the control cohorts were also small. We anticipate that the H3N2b levels in type I and III patients will be higher and lower, respectively, than in type II patients. The cutoffs for normal may be amended after analysis of type III samples as their values may be below the cutoffs established in this study. Second, we were able to collect urine samples from only 2 treated cats, and this sample size was not sufficient to assess the change of urine H3N2b in treated cats. Third, no covariate-adjusted analysis was performed as the sample sizes were too small after samples were matched for patient demographics, and weight and sex of cats. Lastly, only one participant was enrolled in the expanded access study, thus no statistics can be used. This patient was used as her own control to evaluate the pre- and post-treatment efficacy. Although these limitations need to be considered, this study did identify H3N2b as a reliable pharmacodynamic biomarker for gene therapy.

H3N2b offers an expanded dynamic range to evaluate treatment efficacy compared to GM1 gangliosides, which were elevated less than two-fold in plasma and were not elevated at all in CSF of GM1 gangliosidosis patients compared to controls. In fact, it is important to note that patient CSF has no elevation of GM1 ganglioside but ~18-fold increases in H3N2b, which will require future investigations of H3N2b's role in pathogenesis. Notably, H3N2b is readily quantified in biofluids such as urine, plasma, and CSF, making it an ideal non-invasive biomarker for serially monitoring response to treatment. These features will facilitate use of H3N2b as a pharmacodynamic biomarker in gene therapy trials for GM1 gangliosidosis. It is also possible that H3N2b could serve as pharmacodynamics biomarker beyond gene therapy for treatments targeted at augmenting β-galactosidase activity,[2,3] such as marrow transplantation,[36] pharmacological chaperones,[37] and enzyme replacement therapy.[38,39]

Contributors

PK and SM prepared samples for development and validation of assays for H3N2b and for analysis of patient and cat plasma, CSF, and urine samples. RS prepared samples for biomarker discovery and structural identification of H3N2a and H3N2b. MQ performed the last steps of synthesis of H3N2b and d_6-H3N2b and NMR analysis of synthetic intermediates. PD collected samples from GM1 gangliosidosis natural history study and expanded access AAV gene therapy study, and R-E N processed samples and contributed to preparation of the manuscript. ALG, MSE, DRM and HLG-E treated GM1 gangliosidosis cats with AAV gene therapy, collected cat CNS tissues, performed assays for enzymatic activity in cat tissues, and contributed to preparation of the manuscript and investigational new drug application for the expanded access study. DJD collected samples from control subjects and contributed to preparation of the manuscript. MS performed the NMR analysis of H3N2b and d_6-H3N2b. JL performed the statistical analysis and contributed to preparation of the manuscript. CJT designed and supervised GM1 gangliosidosis natural history study and expanded access study and contributed to preparation of the manuscript. CJT, JES, DSO, and XJ designed the studies and wrote the manuscript. XJ also performed mass spectrometry experiments, synthesis of all the intermediates to H3N2b and d_6-H3N2b, and purification of H3N2b and d_6-H3N2b.

Data sharing statement

All data are available in the main text or the supplementary materials. This study includes no data deposited in external repositories.

Declaration of interests

DSO and XJ are named as co-inventors on a patent application pertaining to use of pentasaccharide biomarkers in GM1 gangliosidosis. ALG, DRM, HLG-E and MSE are beneficiaries of a prior licensing agreement with Sio Gene Therapies (New York, New York). DRM and MSE are shareholders in Lysogene (Neuilly-sur-Seine, France).

Acknowledgements

This work was supported by grants from the National Tay-Sachs and Allied Diseases Association Inc (XJ) and the NIH: U01NS114156 (XJ), R01HD060576 (DRM, MSE), and National Human Genome Research Institute Intramural Program ZIAHG200409 (CJT). This work was also supported by the Metabolomics Facility at Washington University (NIH P30 DK020579). We are grateful to the National Tay-Sachs and Allied

Diseases Association Inc for their assistance in obtaining samples from GM1 gangliosidosis subjects.

Appendix A. Supplementary data

Supplementary data related to this article can be found at https://doi.org/10.1016/j.ebiom.2023.104627.

References

1 Johnson WG. Chapter 34: β-galactosidase deficiency: GM1 gangliosidosis, Morquio B disease, and galactosialidosis. In: *Rosenberg's molecular and genetic basis of neurological and psychiatric disease 5th edition roger rosenberg juan pascual*. Elsevier; 2015:385–394.
2 Nicoli ER, Annunziata I, d'Azzo A, Platt FM, Tifft CJ, Stepien KM. GM1 gangliosidosis-A mini-review. *Front Genet*. 2021;12:734878.
3 Rha AK, Maguire AS, Martin DR. GM1 gangliosidosis: mechanisms and management. *Appl Clin Genet*. 2021;14:209–233.
4 Brunetti-Pierri N, Scaglia F. GM1 gangliosidosis: review of clinical, molecular, and therapeutic aspects. *Mol Genet Metab*. 2008;94(4):391–396.
5 McCurdy VJ, Johnson AK, Gray-Edwards HL, et al. Sustained normalization of neurological disease after intracranial gene therapy in a feline model. *Sci Transl Med*. 2014;6(231):231ra48.
6 Gray-Edwards HL, Maguire AS, Salibi N, et al. 7T MRI predicts amelioration of neurodegeneration in the brain after AAV gene therapy. *Mol Ther Methods Clin Dev*. 2020;17:258–270.
7 Gross AL, Gray-Edwards HL, Bebout CN, et al. Intravenous delivery of adeno-associated viral gene therapy in feline GM1 gangliosidosis. *Brain*. 2022;145(2):655–669.
8 Group. F-NBW. *BEST (biomarkers, EndpointS, and other tools) resource*. Silver Spring (MD): Food and Drug Administration (US); Bethesda (MD): National Institutes of Health (US); 2016. www.ncbi.nlm.nih.gov/books/NBK326791/.
9 US Department of Health and Human Services, Food and Drug Administration, Center for Drug Evaluation and Research and Center for Veterinary Medicine. *Guidance for industry: bioanalytical method validations*. 2018.
10 Leonard M, Dunn J, Smith G. A clinical biomarker assay for the quantification of d3-creatinine and creatinine using LC-MS/MS. *Bioanalysis*. 2014;6(6):745–759.
11 Gray-Edwards HL, Jiang X, Randle AN, et al. Lipidomic evaluation of feline neurologic disease after AAV gene therapy. *Mol Ther Methods Clin Dev*. 2017;6:135–142.
12 Gray-Edwards HL, Regier DS, Shirley JL, et al. Novel biomarkers of human GM1 gangliosidosis reflect the clinical efficacy of gene therapy in a feline model. *Mol Ther*. 2017;25(4):892–903.
13 Su P, Khaledi H, Waggoner C, Gelb MH. Detection of GM1-gangliosidosis in newborn dried blood spots by enzyme activity and biomarker assays using tandem mass spectrometry. *J Inherit Metab Dis*. 2021;44(1):264–271.
14 Ramsay SL, Meikle PJ, Hopwood JJ, Clements PR. Profiling oligosaccharidurias by electrospray tandem mass spectrometry: quantifying reducing oligosaccharides. *Anal Biochem*. 2005;345(1):30–46.
15 Piraud M, Pettazzoni M, Menegaut L, et al. Development of a new tandem mass spectrometry method for urine and amniotic fluid screening of oligosaccharidoses. *Rapid Commun Mass Spectrom*. 2017;31(11):951–963.
16 Bonesso L, Piraud M, Caruba C, Van Obberghen E, Mengual R, Hinault C. Fast urinary screening of oligosaccharidoses by MALDI-TOF/TOF mass spectrometry. *Orphanet J Rare Dis*. 2014;9:19.
17 Klein A, Lebreton A, Lemoine J, Perini JM, Roussel P, Michalski JC. Identification of urinary oligosaccharides by matrix-assisted laser desorption ionization time-of-flight mass spectrometry. *Clin Chem*. 1998;44(12):2422–2428.
18 Xia B, Asif G, Arthur L, et al. Oligosaccharide analysis in urine by maldi-tof mass spectrometry for the diagnosis of lysosomal storage diseases. *Clin Chem*. 2013;59(9):1357–1368.
19 Anumula KR. Single tag for total carbohydrate analysis. *Anal Biochem*. 2014;457:31–37.
20 Bruggink C, Wuhrer M, Koeleman CA, et al. Oligosaccharide analysis by capillary-scale high-pH anion- exchange chromatography with on-line ion-trap mass spectrometry. *J Chromatogr B Analyt Technol Biomed Life Sci*. 2005;829(1-2):136–143.
21 Spengler B, Kirsch D, Kaufmann R. Structure analysis of branched oligosaccharides using post-source decay in matrix-assisted laser desorption ionization mass spectrometry. *J Mass Spectrom*. 1995;30:782–787.
22 Lemoine J, Fournet B, Despeyroux D, Jennings KR, Rosenberg R, de Hoffmann E. Collision-induced dissociation of alkali metal cationized and permethylated oligosaccharides: influence of the collision energy and of the collision gas for the assignment of linkage position. *J Am Soc Mass Spectrom*. 1993;4(3):197–203.
23 Michalski JC, Strecker G, van Halbeek H, Dorland L, Vliegenthart JF. The structures of six urinary oligosaccharides that are characteristic for a patient with Morquio syndrome type B. *Carbohydr Res*. 1982;100:351–363.
24 Wu Z, Liu Y, Li L, et al. Decoding glycan protein interactions by a new class of asymmetric N-glycans. *Org Biomol Chem*. 2017;15(42):8946–8951.
25 Arnarp J, Lönngren J. Synthesis of a tri-, a penta-, and a heptasaccharide containing terminal N-acetyl-β-D- lactosaminyl residues, part of the 'complex-type' carbohydrate moiety of glycoproteins. *J Chem Soc Perkin Trans I*. 1981:2070–2074.
26 Khamis MM, Adamko DJ, El-Aneed A. Strategies and challenges in method development and validation for the absolute quantification of endogenous biomarker metabolites using liquid chromatography-tandem mass spectrometry. *Mass Spectrom Rev*. 2021;40(1):31–52.
27 Regier DS, Tifft CJ, Rothermel CE. GLB1-Related disorders [Updated 2021 Apr 22]. In: Adam MP, Ardinger HH, Pagon RA, et al., eds. *GeneReviews®*. Seattle (WA): University of Washington, Seattle; 2013:1993–2021. Table 2. [β-Galactosidase Enzyme Activity in GLB1-Related Disorders by Phenotype]. Available from: https://www.ncbi.nlm.nih.gov/books/NBK164500/table/gm1-ganglio.T._galactosidase_enzyme_acti/.
28 Utz JR, Crutcher T, Schneider J, Sorgen P, Whitley CB. Biomarkers of central nervous system inflammation in infantile and juvenile gangliosidoses. *Mol Genet Metab*. 2015;114(2):274–280.
29 Regier DS, Kwon HJ, Johnston J, et al. MRI/MRS as a surrogate marker for clinical progression in GM1 gangliosidosis. *Am J Med Genet A*. 2016;170(3):634–644.
30 Harden A, Martinovic Z, Pampiglione G. Neurophysiological studies in GM1, gangliosidosis. *Ital J Neurol Sci*. 1982;3(3):201–206.
31 Pampiglione G, Harden A. Neurophysiological investigations in GM1 and GM2 gangliosidoses. *Neuropediatrics*. 1984;15(Suppl):74–84.
32 Kilic M, Kasapkara CS, Kilavuz S, Mungan NO, Biberoglu G. A possible biomarker of neurocytolysis in infantile gangliosidoses: aspartate transaminase. *Metab Brain Dis*. 2019;34(2):495–503.
33 Lawrence R, Van Vleet JL, Mangini L, et al. Characterization of glycan substrates accumulating in GM1 Gangliosidosis. *Mol Genet Metab Rep*. 2019;21:100524.
34 Satoh H, Yamato O, Asano T, et al. Cerebrospinal fluid biomarkers showing neurodegeneration in dogs with GM1 gangliosidosis: possible use for assessment of a therapeutic regimen. *Brain Res*. 2007;1133(1):200–208.
35 Wajner A, Michelin K, Burin MG, et al. Comparison between the biochemical properties of plasma chitotriosidase from normal individuals and from patients with Gaucher disease, GM1-gangliosidosis, Krabbe disease and heterozygotes for Gaucher disease. *Clin Biochem*. 2007;40(5-6):365–369.
36 Shield JP, Stone J, Steward CG. Bone marrow transplantation correcting beta-galactosidase activity does not influence neurological outcome in juvenile GM1-gangliosidosis. *J Inherit Metab Dis*. 2005;28(5):797–798.
37 Suzuki Y. Chaperone therapy update: fabry disease, GM1-gangliosidosis and Gaucher disease. *Brain Dev*. 2013;35(6):515–523.
38 Kelly JM, Gross AL, Martin DR, Byrne ME. Polyethylene glycol-b-poly(lactic acid) polymersomes as vehicles for enzyme replacement therapy. *Nanomedicine*. 2017;12(23):2591–2606.
39 Condori J, Acosta W, Ayala J, et al. Enzyme replacement for GM1-gangliosidosis: uptake, lysosomal activation, and cellular disease correction using a novel beta-galactosidase:RTB lectin fusion. *Mol Genet Metab*. 2016;117(2):199–209.